The Journal of Immunology

Multifunctional NK Cell–Engaging Antibodies Targeting EGFR and NKp30 Elicit Efficient Tumor Cell Killing and Proinflammatory Cytokine Release

Katja Klausz, Lukas Pekar, Ammelie Svea Boje, Carina Lynn Gehlert, Steffen Krohn, Tushar Gupta, Yanping Xiao, Simon Krah, Rinat Zaynagetdinov, Britta Lipinski, Lars Toleikis, Sven Poetzsch, Brian Rabinovich, Matthias Peipp and Stefan Zielonka

J Immunol published online 14 September 2022
http://www.jimmunol.org/content/early/2022/09/14/jimmunol.2100970

Supplementary Material **http://www.jimmunol.org/content/suppl/2022/09/14/jimmunol.2100970.DCSupplemental**

The Journal of Immunology is published twice each month by The American Association of Immunologists, Inc., 1451 Rockville Pike, Suite 650, Rockville, MD 20852

Print ISSN: 0022-1767 Online ISSN: 1550-6606.

Published September 14, 2022, doi:10.4049/jimmunol.2100970

Multifunctional NK Cell–Engaging Antibodies Targeting EGFR and NKp30 Elicit Efficient Tumor Cell Killing and Proinflammatory Cytokine Release

Katja Klausz,*,[1] Lukas Pekar,†,[1] Ammelie Svea Boje,*,[1] Carina Lynn Gehlert,* Steffen Krohn,* Tushar Gupta,‡ Yanping Xiao,§ Simon Krah,† Rinat Zaynagetdinov,§ Britta Lipinski,†,¶ Lars Toleikis,† Sven Poetzsch,‖ Brian Rabinovich,§ Matthias Peipp,*,[2] and Stefan Zielonka†,¶,[2]

In this work, we have generated novel Fc-comprising NK cell engagers (NKCEs) that bridge human NKp30 on NK cells to human epidermal growth factor receptor (EGFR) on tumor cells. Camelid-derived VHH single-domain Abs specific for human NKp30 and a humanized Fab derived from the EGFR-specific therapeutic Ab cetuximab were used as binding arms. By combining camelid immunization with yeast surface display, we were able to isolate a diverse panel of NKp30-specific VHHs against different epitopes on NKp30. Intriguingly, NKCEs built with VHHs that compete for binding to NKp30 with B7-H6, the natural ligand of NKp30, were significantly more potent in eliciting tumor cell lysis of EGFR-positive tumor cells than NKCEs harboring VHHs that target different epitopes on NKp30 from B7-H6. We demonstrate that the NKCEs can be further improved with respect to killing capabilities by concomitant engagement of FcγRIIIa and that soluble B7-H6 does not impede cytolytic capacities of all scrutinized NKCEs at significantly higher B7-H6 concentrations than observed in cancer patients. Moreover, we show that physiological processes requiring interactions between membrane-bound B7-H6 and NKp30 on NK cells are unaffected by noncompeting NKCEs still eliciting tumor cell killing at low picomolar concentrations. Ultimately, the NKCEs generated in this study were significantly more potent in eliciting NK cell–mediated tumor cell lysis than cetuximab and elicited a robust release of proinflammatory cytokines, both features which might be beneficial for antitumor therapy. ***The Journal of Immunology*****, 2022, 209: 1–12.**

Natural killer cells are innate immune cells that play a pivotal role in early host defense against infections and tumors (1, 2). NK cells were first described in the 1970s based on their ability to exert antitumor cell cytotoxicity without prior sensitization (3, 4). In contrast to T cells that recognize distinct Ags via a variable TCR, the discrimination between healthy and stressed cells and consequently the antitumor responses of NK cells is based on a sophisticated interplay between a multitude of germline-encoded activating and inhibitory receptors (3, 5). Inhibitory receptors include killer Ig-like receptors, ILT2/4, or NKG2A that recognize "safe" or "self" ligands (1, 6). On the contrary, receptors triggering NK cell activation upon binding of ligands that are upregulated on stressed cells include the natural cytotoxicity receptors NKp30, NKp44, and NKp46 as well as NKG2D, 2B4, and DNAM-1 (7, 8). Interestingly, shedding of ligands for NK cell–activating receptors such as B7-H6, MICA/B, or Galectin-3 have been described as mechanisms of tumor immune escape (5, 9–11). Moreover, NK cell–mediated immune editing of tumor cells (e.g., melanoma) may select for MHC class I^{hi} and NKG2D $ligand^{lo}$ variants that evade NK cell and possibly T cell recognition (12).

Another mechanism of NK cell activation is mediated by low-affinity FcγRIIIa or CD16a that is expressed on NK cells. FcγRIIIa engagement by an IgG Ab bound to its target cell induces potent NK cell degranulation and is a major pathway by which NK cells are directed to "foreign" Ag expression in infections and tumors (13). This killing process termed Ab-dependent cell-mediated cytotoxicity (ADCC) is considered as one important mode of action of many therapeutic IgG1 Abs, including cetuximab (14, 15). The capability of an Ab to elicit ADCC, however, is impacted by multiple factors including target Ag density, FcγRIIIa polymorphisms (in humans), FcγRIIIa downregulation and shedding, as well as competition for binding to FcγRIIIa with circulating endogenous IgG (7, 15–19). In addition, less differentiated $CD56^{hi}$ or dysfunctional $CD56^{lo}$ FcγRIIIa-negative NK cells might be enriched in tumor-

*Division of Antibody-Based Immunotherapy, Department of Internal Medicine II, University Hospital Schleswig-Holstein and Christian Albrechts University Kiel, Kiel, Germany; †Protein Engineering and Antibody Technologies, Merck Healthcare KGaA, Darmstadt, Germany; ‡Protein Engineering and Antibody Technologies, EMD Serono Research & Development Institute, Inc., Billerica, MA; §Department of Oncology and Immuno-oncology, EMD Serono Research & Development Institute, Inc., Billerica, MA; ¶Institute for Organic Chemistry and Biochemistry, Technical University of Darmstadt, Darmstadt, Germany; and ‖Strategic Innovation, Merck Healthcare KGaA, Darmstadt, Germany

[1]K.K., L.P., and A.S.B. contributed equally to this work.

[2]M.P. and S.Z. contributed equally to this work as cosenior authors.

ORCIDs: 0000-0001-9259-0965 (L.P.), 0000-0001-8895-2441 (T.G.), 0000-0001-6476-3523 (B.L.), 0000-0002-3579-7203 (S.P.).

Received for publication October 8, 2021. Accepted for publication August 23, 2022.

Address correspondence and reprint requests to Prof. Matthias Peipp or Dr. Stefan Zielonka, Division of Antibody-Based Immunotherapy, Department of Internal Medicine II, University Hospital Schleswig-Holstein and Christian Albrechts University Kiel, Rosalind-Franklin-Strasse 12, 24105 Kiel, Germany (M.P.) or Protein Engineering and Antibody Technologies, Merck Healthcare KGaA, Frankfurter Strasse 250, 64293 Darmstadt, Germany (S.Z.). E-mail addresses: matthias.peipp@uksh.de (M.P.) or stefan.zielonka@merckgroup.com (S.Z.)

The online version of this article contains supplemental material.

Abbreviations used in this article: ADCC, Ab-dependent cell-mediated cytotoxicity; CHO, Chinese hamster ovary; ECD, extracellular domain; EGFR, epidermal growth factor receptor; KB, kinetics buffer; MNC, mononuclear cell; NKCE, NK cell engager; rh, recombinant human; NSCLC, non–small cell lung cancer; SEC, size-exclusion chromatography.

infiltrating NK cell populations (e.g., non–small cell lung cancer), greatly diminishing ADCC (20, 21).

In recent years, redirection and conditional activation of NK cells at the tumor site evolved as a promising approach for cancer immunotherapy, and currently several different molecules are being investigated in clinical trials (22, 23). In this respect, bispecific and multispecific NK cell engagers (NKCEs) have been developed, in which one paratope binds to the activating FcγRIIIa with high affinity, whereas the other paratope is directed against a tumor-associated Ag (24–26). In 2019, Vivier and colleagues (27) described the efficient generation of trifunctional NKCEs. In their work, the authors employed two activating receptors of NK cells, NKp46 as well as FcγRIIIa, for effector cell engagement and could show more potent antitumor activity than clinically approved Abs targeting the same Ag, but solely triggering FcγRIIIa. In another work by Kerfelec and colleagues (28), HER2 as well as NKG2D-targeting single-domain Abs (sdAbs) were exploited for the generation of bispecific NKCEs mediating tumor cell–directed cytotoxicity as well as release of TNF-α. Besides conventional bispecific and multispecific NKCE triggering various NK cell receptors, molecules harboring cytokines have also been realized and show promising activities in preclinical models and initial clinical trials (22, 29). An additional way of conditionally agonizing NK cells relies on the generation of bifunctional or multifunctional immunoligands (30–32). Immunoligands are fusion proteins composed of an Ab-derived arm for tumor cell targeting and a natural ligand for an activating receptor on the immune cell population, thereby inducing effector cell redirection and activation against tumor cells. Recently, we were able to show that tumor cells can be efficiently lysed by EGFR-targeting and NKp30-activating immunoligands based on affinity-optimized versions of B7-H6 (33). NKp30 is an activating receptor on most NK cells (34), subsets of $CD8^+$ T cells (35), and stimulated $V\delta1^+$ T cells (36). The engineered B7-H6–derived immunoligands in this study promoted NK cell–mediated tumor cell lysis by NKp30 engagement comparable to therapeutic IgG1 Ab cetuximab activating NK cells via FcγRIIIa, but they intriguingly provoked a more prominent release of proinflammatory cytokines TNF-α and IFN-γ (33).

In the current study, NKp30-specific VHH sdAbs were generated by immunization of camelids followed by yeast surface display (37, 38). A diverse panel of VHHs targeting different epitopes on human NKp30 was isolated. After reformatting into bispecific Ab derivatives harboring a humanized Fab derived from the therapeutic EGFR-targeting Ab cetuximab (hu225) for tumor cell targeting, resulting NKCEs (referred to as VHH SEEDbodies) triggered efficient elimination of EGFR-positive tumor cells of different origins. Interestingly, NKCEs harboring VHHs competing with the natural ligand B7-H6 for binding on NKp30 were significantly more potent in inducing tumor cell lysis than noncompeting molecules binding other epitopes on NKp30. Soluble B7-H6 at substantially higher concentrations than shed B7-H6 found in cancer patients did not impede cytolytic capabilities of all tested NKCEs. However, NKCEs based on B7-H6 competing VHHs interfere with the physiological B7-H6/NKp30 axis, whereas VHH SEEDbodies harboring noncompeting sdAbs do not significantly alter this interaction, a feature that might render them attractive as therapeutic agents. Moreover, we were able to show that killing capacities of VHH SEEDbodies can be further enhanced by concomitant engagement of FcγRIIIa and NKp30 on NK cells exploiting an immune effector-competent IgG1 Fc backbone. Intriguingly, release of IFN-γ and TNF-α by triggering NKp30 was increased for most analyzed NKCEs compared with FcγRIIIa activation by the therapeutic Ab cetuximab. Taken together, these functional characteristics combined with preferred developability attributes highlight the potential of VHH-harboring NKCEs activating NK cells via NKp30 as valuable molecules for cancer immunotherapy.

Materials and Methods

Immunization of camelids

Three camelids, that is, one llama (*Lama glama*), one alpaca (*Vicugna pacos*), and one huarizo (*Lama glama* × *Vicugna pacos*), were immunized with recombinant human (rh)NKp30 extracellular domain (ECD; produced in-house at Merck Healthcare KGaA) at preclinics (Potsdam, Germany). All procedures and animal care were in accordance with local animal welfare protection laws and regulations. In brief, 200 μg of rhNKp30 diluted in 1 ml of PBS was either emulsified with 1 ml of CFA (initial immunization) or IFA (subsequent immunizations). Administrations were performed s.c. at three sites. A total of six immunizations (days 0, 28, 42, 56, 70, and 84) were performed during the course of 84 d. On day 88, a volume of 100 ml of blood was collected, total RNA was extracted, and cDNA was synthesized. All animals in this study were provided by preclinics and remained alive after completion of the immunization procedure.

Yeast strains and media

For yeast surface display, *Saccharomyces cerevisiae* strain EBY100 (*MATa URA3-52 trp1 leu2Δ1 his3Δ200 pep4::HIS3 prb1Δ1.6R can1 GAL* (*pIU211:URA3*)) (Thermo Fisher Scientific) was used. Cells were cultivated in YPD medium composed of 20 g/l peptone, 20 g/l dextrose, and 10 g/l yeast extract supplemented with 10 mg/ml penicillin-streptomycin (Life Technologies). Cells harboring library plasmids (pDisp) after homologous recombination-based cloning were cultivated in medium using minimal SD-base (Takara Bio) with commercially available dropout mix (Takara Bio) composed of all essential amino acids except for tryptophan (−Trp), according to the manufacturer's instructions, supplemented with 5.4 g/l Na_2HPO_4 and 8.6 g/l $NaH_2PO_4 \times H_2O$. For induction of Ab gene expression, cells were transferred into SG dropout medium (−Trp) wherein glucose was replaced by galactose containing SG-base medium (Takara Bio) supplemented with 10% (w/v) polyethylene glycol 8000 (PEG 8000).

Plasmids for yeast surface display and library generation

Homologous recombination in yeast, referred to as gap repair cloning, was exploited for the generation of VHH sublibraries. Protocols for PCR amplification of VHH fragments as well as library construction have already been described by our group (37). In short, display plasmid pDisp was digested with BsaI followed by genetic fusion of VHH library candidates in frame to Aga2p by replacement of a stuffer sequence due to gap repair cloning, ultimately enabling surface presentation of sdAb variants on yeast cell surface. Furthermore, insertion of a hemagglutinin epitope linked to the C terminus of Aga2p allowed for the detection of full-length VHHs on the yeast surface (Fig. 1A).

Library sorting

For library sorting, His-tagged rhNKp30 ECD was purchased from Abcam. EBY100 library cells were grown overnight in SD medium with dropout mix lacking tryptophan (−Trp) at 30°C and 120 rpm. For induction of surface expression, cells were transferred into SG medium with dropout mix (−Trp) at 10^7 cells/ml followed by a 48 h incubation at 20°C. Ag binding was monitored by indirect immunofluorescence using His-tagged NKp30 ECD followed by applying an anti-His mouse monoclonal detection Ab (SureLight allophycocyanin, Abcam, diluted 1:20). Full-length VHH surface expression was detected simultaneously by hemagglutinin epitope labeling utilizing a FITC-labeled rabbit polyclonal Ab (Abcam, diluted 1:20). For the detection and isolation of library candidates, a BD FACSAria Fusion cell sorter (BD Biosciences) was employed. Control samples, that is, untreated cells, cells incubated with labeling reagents only or cells incubated with labeling reagents, and His-tagged NKp30 or unrelated Ags, were employed in every experiment, allowing for gate adjustment of the desired cell population.

Protein expression and purification

After sequencing and VHH clone selection, variants were fused to the hinge region of the SEED AG chain and cloned into pTT5 allowing for bispecific SEEDbody production in combination with humanized cetuximab Fab (hu225) on the SEED GA chain (Fig. 1A). SEEDbodies were either produced with a wild-type IgG1 CH2 domain (effector competent, VHH SEEDbody eff+) or in an effector-silenced backbone (VHH SEEDbody eff−). To this end, Expi293 cells were transfected with respective expression vectors according to the manufacturer's instructions (Thermo Fisher Scientific).

At 5 d posttransfection, supernatants were harvested by centrifugation and purified via MabSelect Ab purification chromatography resin (GE Healthcare). Finally, buffer was exchanged to PBS (pH 6.8) overnight using a Pur-A-Lyzer Maxi 3500 dialysis kit (Sigma-Aldrich). Concentrations were determined using NanoDrop ND-1000 (Peqlab) after sterile filtration with Ultrafree-CL GV 0.22 μm centrifugal devices (Merck Millipore). Sample purities were assessed by determining target monomer peaks (%) via analytical size-exclusion chromatography (SEC) using 10 μg of protein per sample on a TSKgel SuperSW3000 column (4.6 × 300 mm, Tosoh Bioscience) in an Agilent HPLC system with a flow rate of 0.35 ml/min. An ECD of B7-H6 was designed in-house at Merck Healthcare KGaA as polyhistidine-tagged protein, synthesized, and subcloned into pTT5 plasmid backbone at GeneArt (Thermo Fisher Scientific) for transient expression in Expi293 cells and expressed according to the Ab molecules, except using a larger production volume of 400 ml. Downstream processing for the ECD was conducted as two-step purification, starting with immobilized metal affinity chromatography using a HisTrap 5 ml column (GE Healthcare) and nickel sulfate at a final concentration of 1 mM. After sample load and washout, the protein was eluted with an imidazole gradient from 20 to 500 mM. Target-containing fractions were pooled and further processed in a preparative SEC. To this end, a HiLoad 26/600 Superdex 75-pg column (26 × 600 mm, Merck) in an Agilent HPLC system was used to pool the B7-H6-His ECD containing fractions based on elution profile prior to sterile filtration.

Biolayer interferometry

The Octet RED96 system (ForteBio, Pall Life Sciences) was employed for kinetic measurements as well as competition assays at 25°C and 1000 rpm agitation. For binding kinetic measurements, bispecific VHH SEEDbodies were loaded on anti-human Fc biosensors at 5 μg/ml in PBS for 3 min followed by 60 s sensor rinsing in kinetics buffer (KB; PBS + 0.1% Tween 20 and 1% BSA). Afterwards, association to the human NKp30 ECD (Abcam) in varying concentrations ranging from 6.25 to 200 nM in KB was measured for 300 s, followed by dissociation for 300 s in KB. In each experiment, one negative control was measured using irrelevant Ag. Moreover, one reference value was measured incubating the Ab in KB instead of the Ag. To analyze competition for binding to NKp30 with the natural ligand B7-H6, NKp30 was loaded at 3 μg/ml in PBS for 3 min to anti-His tips (HIS1K) followed by 60 s sensor rinsing in KB. Association of the VHH SEEDbodies (200 nM) was conducted for 300 s in KB, followed by an additional association step for 60 s with the natural ligand B7-H6 (500 nM, expressed as SEEDbody fusion) in KB. Epitope binning experiments of VHH SEEDbodies were conducted similarly except for using 200 nM for both VHH SEEDbody association steps for 180 s (first association) and 120 s (second association) in KB.

Data were fitted and analyzed with ForteBio data analysis software 8.0 using a 1:1 binding model after Savitzky–Golay filtering.

Cell culture

EGFR-expressing tumor cell lines A431, A549, SW-480, HCT116, and H2030 were obtained from American Type Culture Collection. A431 cells were cultured in RPMI 1640 GlutaMAX-I supplemented with 10% FCS, 100 U/ml penicillin, and 100 mg/ml streptomycin (R10+). A549, SW-480, and H2030 were cultured in DMEM supplemented with 10% FCS, 100 U/ml penicillin, and 100 mg/ml streptomycin (D10+; all components from Thermo Fisher Scientific), and HCT116 cells were cultivated in McCoy's culture medium supplemented with 10% FCS, 100 U/ml penicillin, and 100 mg/ml streptomycin. Additionally, Chinese hamster ovary cells (ExpiCHO-S, Thermo Fisher Scientific) were cultivated in suspension with complete ExpiCHO expression medium. To generate CHO-S cells expressing human B7-H6, 2×10^8 cells were transiently transfected by flow electroporation (MaxCyte STx system) in OC-100 cuvettes with 120 μg of human NK cell cytotoxicity receptor 3 ligand 1 (NCR3LG1, B7-H6) mammalian expression plasmid (Sino Biological) and cultured in CD OptiCHO medium (Thermo Fisher Scientific). After 48 h, human B7-H6 expression was analyzed by flow cytometry using 50 μg/ml anti-human B7-H6 mouse IgG1 Ab (R&D Systems) and anti-mouse IgG whole-molecule $F(ab')_2$ fragment–FITC (1:20; Sigma-Aldrich) on a Navios EX flow cytometer (Beckman Coulter).

Tumor cell killing assays

Experiments were approved by the Ethics Committee of Christian Albrechts University of Kiel (Kiel, Germany) and in accordance with Merck internal guidelines and with the Declaration of Helsinki. Preparation of mononuclear cells (MNCs) from healthy donors was performed as previously described after receiving written informed consent (39). NK cells were isolated by negative selection using an NK cell isolation kit (Miltenyi Biotec) and maintained overnight at a density of 2×10^6 cells/ml in R10+ medium. Cytotoxicity was analyzed in standard 4 h ^{51}Cr-release assays performed in 96-well microtiter plates in a total volume of 200 μl as described previously (39). Human MNCs or purified NK cells were used as effector cells at E:T ratios of 40:1 and 10:1, respectively. VHH SEEDbodies and cetuximab were applied at the concentrations indicated. In selected experiments, NK cells were labeled with ^{51}Cr to analyze fratricide/activation-induced cell death.

To investigate potential inhibitory effects of the natural NKp30 ligand B7-H6 on NK cell–mediated tumor cell lysis by NKCEs, cytotoxicity assays were performed in the presence of 5 μg/ml (178.6 nM) B7-H6 ECD-His (produced in-house) and VHH SEEDbodies at saturating concentrations of 5 μg/ml (44.6 nM). Percent lysis was calculated from cpm as follows: % lysis = [(experimental cpm − basal cpm)/(maximal cpm − basal cpm)] × 100.

To analyze whether NK cell–mediated killing by NKp30 and B7-H6 interaction is influenced by VHH SEEDbodies competing or not competing with the B7-H6 binding epitope on NKp30, B7-H6–transfected CHO-S cells were used as target cells together with NK cells in standard 4 h ^{51}Cr-release assays in the presence of increasing concentrations of the indicated NKCEs. The percentage of relative lysis was calculated by using the above formula and normalization (0% = basal release, 100% = % NK cell–mediated lysis without VHH SEEDbody).

For the assessment of NK cell death upon activation or fratricide, additional assays based on fluorescence microscopy were conducted. To this end, PBMCs were isolated from the blood of healthy donors by density gradient centrifugation. Enrichment of NK cells was achieved using the EasySep human NK cell isolation kit (STEMCELL Technologies). Cells were rested overnight in complete medium using low-dose rhIL-2 (100 U/ml, R&D Systems) prior to adjustment to 0.625×10^6 cells/ml. High EGFR-expressing A431 cells were stained with CellTracker Deep Red dye (Thermo Fisher Scientific). Target cells were plated into a 384-well clear bottom microtiter plate (Greiner Bio-One) at 2500 cells/well and incubated for 3 h for adherence. Afterwards, NK cells were added at an E:T ratio of 5:1 and Abs were added at a final concentration of 50 nM. SYTOX Green dead cell stain (Invitrogen, 0.03 μM) was dispensed to the assay followed by plate incubation and on-line measurement for 24 h in the Incucyte system. Lysis was normalized to maximum lysis triggered by target cells cultivated with 30 μM staurosporine (Merck Millipore). Subtraction of overlay signals representing dead tumor cells from overall dead cell signal allowed for analysis of dead NK cells only.

NK cell activation assay

Twenty thousand A431 cells/well were seeded in 96-well V-bottom microtiter plates (Thermo Fisher Scientific) and rested 3 h for adherence before addition of 100,000 NK cells/well (E:T ratio of 5:1), which were treated with 100 U/ml rhIL-2 overnight. Abs were added at a final concentration of 50 nM prior to a 24 h incubation at 37°C. For staining purposes, cells were washed gently with PBS + 1% BSA, followed by incubation with anti-CD56 PE-Cy7 (Beckman Coulter), anti-CD16 AF647 (R&D Systems), and anti-CD107a AF488 (R&D Systems) or respective isotype control Abs for 1 h on ice. Afterwards, cells were washed and measured via flow cytometry exploiting the IntelliCyt iQue Screener Plus system (Sartorius). Measurement and compensation of fluorochromes were performed with IntelliCyt ForeCyt enterprise client edition version 8.0.7430 software (Sartorius). The applied gating strategy is shown in Supplemental Fig. 2.

AKT pathway signaling assay

A549 cells were seeded to a final cell density of 1×10^5 cells/well into sterile cell culture 96-well plates with complete growth medium. After adherence, cells were serum starved overnight. On the next day, cells were treated using decreasing Ab (1:4 dilution) concentrations with a maximum of 2.5 μM for 1 h in serum-free medium prior to the stimulation of downstream signaling utilizing 10 ng/ml rhEGF solution for 10 min at 37°C. Afterwards, the supernatant was removed and the A549 cells were lysed using lysis buffer from phospho-AKT1/2/3 (Ser^{473}) HTRF kit (Cisbio). Subsequent phosphoprotein analysis was performed and measured following the manufacturer's protocol.

Cytokine release assay

Quantification of IFN-γ and TNF-α released by NK cells was performed using human cytokine HTRF kits (Cisbio) as described earlier (33). In brief, 2500 EGFR-positive A431 cells per well were seeded in 384 clear-bottom microtiter plates (Greiner Bio-One) and incubated for 3 h. Following an overnight incubation in complete medium containing 100 U/ml rhIL-2 (R&D Systems), 12,500 NK cells were added, resulting in an E:T ratio of 5:1. VHH SEEDbodies were added to a final concentration of 50 nM. As controls, tumor cells alone as well as NK cells cultivated with tumor cells in the absence of NKCEs were used. After a 24 h incubation, cells were sedimented by centrifugation, and cytokine-containing supernatants were further processed according to the manufacturer's instructions. Assay plates were

measured with a PHERAstar FSX device (BMG Labtech). HTRF optical entity using excitation at 337 nm and emission at 620 nm as well as 665 nm was used. Analyses and fitting of resulting data were facilitated by MARS software (v3.32, BMG) enabling a four-parameter logistic (4PL $1/y^2$) model fitting of the standard curve following the kit manufacturer's instructions.

Data processing and statistical analysis

Graphical and statistical analyses were performed with GraphPad Prism 8 software. The *p* values were calculated employing repeated measures ANOVA and the Bonferroni or Tukey posttest as recommended, or the Student *t* test when appropriate. A *p* value of ≤ 0.05 was regarded as statistically significant.

Results

Selection of a diverse panel of NKp30-specific VHH sdAbs

To generate sdAbs targeting human NKp30, one llama (*Lama glama*), one alpaca (*Vicugna pacos*), and one huarizo (*Lama glama* × *Vicugna pacos*) were immunized with the recombinant ECD of human NKp30 (Fig. 1A). Based on PBMCs derived from whole blood, a yeast surface display library was constructed per animal specimen, resulting in three sublibraries with sizes in the range of $\sim 5 \times 10^8$ independent clones. These libraries were subjected to FACS-based selections (Fig. 1B). To this end, a two-dimensional labeling strategy was exploited to concomitantly detect functional VHH surface expression as well as NKp30 binding (Fig. 1A). In the first round of selection, each sublibrary was sorted separately by FACS using an NKp30 concentration of 1 μM (Fig 1B). Afterwards, the library output was combined for a second selection round with significantly reduced NKp30 concentrations (100 nM) aiming at enhancing selection stringencies (Fig. 1B). Subsequently, 96 clones were sent out for sequencing, resulting in 76 unique clones (Fig. 1C). From clonotyping the selection output based on CDR3 sequence diversity, 18 clones were chosen for reformatting and expressed as bispecific VHH SEEDbodies, with the second arm consisting of a Fab derived from a humanized version of the EGFR-targeting therapeutic Ab cetuximab (hu225) (40, 41). To only focus on NK cell activation via NKp30, an immune effector silenced Fc version was employed (VHH SEEDbodies eff−).

NKp30-specific VHH demonstrate a wide range of affinities and epitope coverage for NKp30, including binders for the same region as natural ligand B7-H6

Besides two SEEDbodies showing no production at all, expression yields for bispecific NKCEs were in the double to triple digit milligram per liter scale. Moreover, aggregation properties as indicated by analytical SEC after protein A purification were favorable, i.e., for most of the molecules above the 90% target peak (Table I).

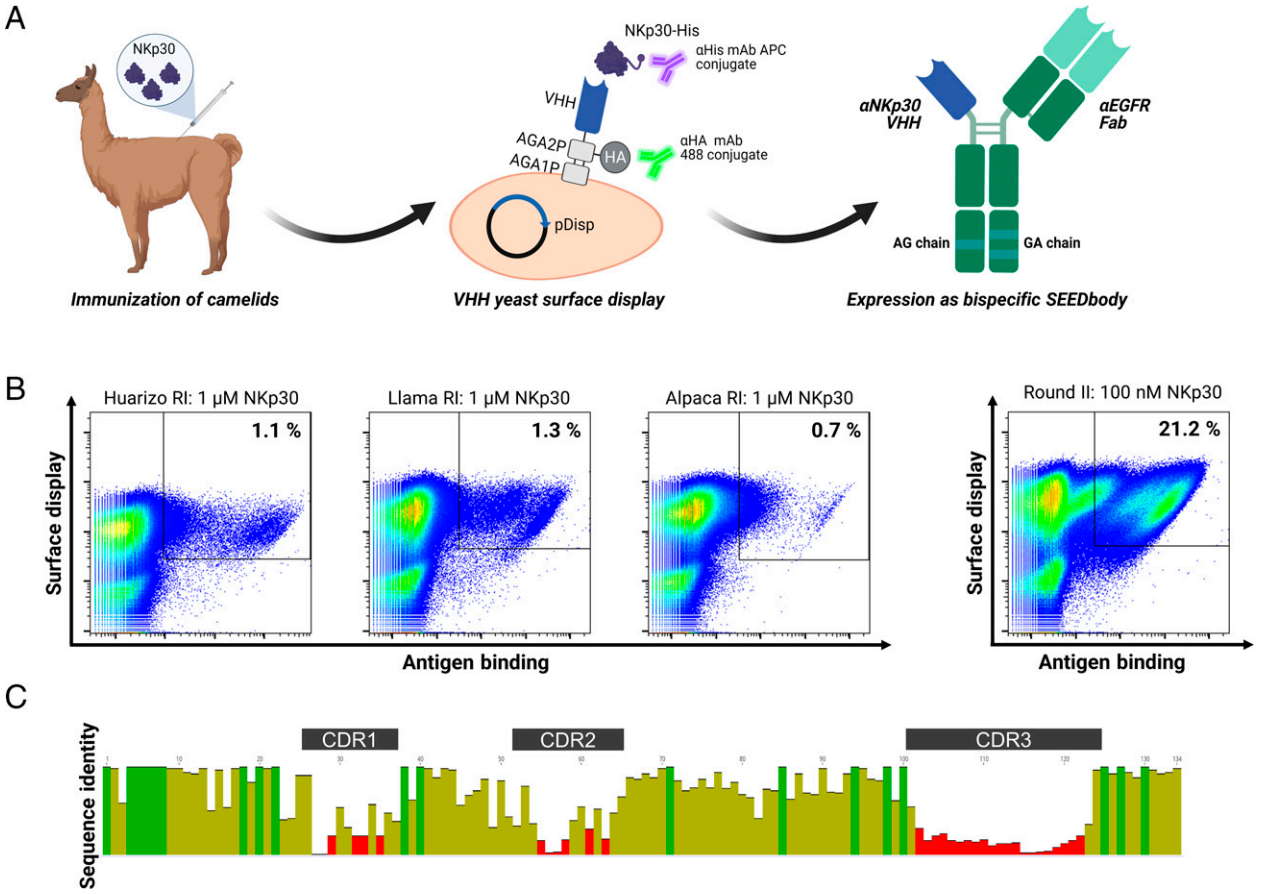

FIGURE 1. Camelid immunization combined with yeast surface display allows for the generation of NKCEs based on NKp30-specific VHH single-domain Abs. (**A**) Scheme depicting the generation of NKp30-targeting VHHs that are used for constructing bispecific NKCEs. After immunization of three camelids with rhNKp30, yeast surface display was employed for the isolation of Ag-specific VHHs. Subsequently, VHHs were incorporated into bispecific SEEDbodies harboring the humanized Fab arm of cetuximab for tumor targeting. For in-depth characterization, Fc-mediated effector functions were silenced by the introduction of the mutations. The scheme was generated using www.biorender.com. (**B**) FACS selection for the isolation of NKp30-specific VHHs by implementing a two-dimensional staining strategy for full-length VHH display and NKp30 binding. Of note, in sorting round one, all three sublibraries based on each immunized specimen were sorted separately, followed by combining the sort one output for the subsequent sorting round two. (**C**) Graphical alignment of 76 unique VHH clones obtained from yeast surface display library sorting. Complementarity-determining regions (CDRs) are indicated. Green bars represent high sequence conservation and red bars indicate high sequence diversity at a given position. Alignment conducted by MUSCLE alignment using Geneious Prime 2021.1.1.

Table I. Biochemical and biophysical characterization of VHH-based EGFR × NKp30 NKCEs

Name	K_D (M)	k_{on} (1/Ms)	k_{off} (1/s)	SEC (%)	Competition with B7-H6	Epitope Bin
VHH1 SEEDbody eff−	2.70E−10	8.19E+05	2.22E−04	88	Yes	I
VHH2 SEEDbody eff−	3.27E−09	1.98E+05	6.46E−04	90	No	III
VHH3 SEEDbody eff−	2.81E−10	6.04E+05	1.70E−04	92	Yes	I
VHH4 SEEDbody eff−	2.57E−09	8.48E+04	2.18E−04	92	Partially	IV
VHH5 SEEDbody eff−	2.89E−10	6.43E+05	1.86E−04	93	Yes	I
VHH6 SEEDbody eff−	2.92E−07	4.42E+05	1.29E−01	93	No	V
VHH7 SEEDbody eff−	5.24E−08	6.72E+04	3.52E−03	86	No	VI
VHH8 SEEDbody eff−	3.22E−10	4.16E+05	1.34E−04	96	No	VII
VHH9 SEEDbody eff−	4.99E−09	3.76E+05	1.87E−03	96	No	VII
VHH10 SEEDbody eff−	2.53E−10	3.46E+05	8.75E−05	91	No	VII
VHH11 SEEDbody eff−	1.02E−09	4.05E+05	4.15E−04	92	No	VII
VHH12 SEEDbody eff−	9.82E−10	9.14E+05	8.98E-04	91	Yes	II
VHH13 SEEDbody eff−	2.11E−10	7.66E+05	1.62E−04	90	Yes	I
VHH14 SEEDbody eff−	3.10E−10	4.64E+05	1.44E−04	97	Yes	I
VHH15 SEEDbody eff−	<1.0E−12	4.40E+05	<1.0E−07	90	Yes	II
VHH16 SEEDbody eff−	1.39E−10	6.66E+05	9.28E−05	91	Yes	I

k_{on} is the rate constant of association and k_{off} is the rate constant of dissociation.

The VHH Abs displayed a broad range of affinities with respect to NKp30 binding, ranging from triple digit nanomolar binding (VHH6 SEEDbody) to affinities in the subnanomolar range (VHH1, VHH3, VHH5, VHH8, VHH10, and VHH12–VHH16 SEEDbodies; Table I). NKp30 epitope specificity and competition of the generated VHH SEEDbodies with the natural ligand B7-H6 for binding to NKp30 was determined via biolayer interferometry (Supplemental Fig. 1). For this, the recombinant NKp30 ECD was captured to the biosensor, and the N-terminal V-like domain of B7-H6 produced as SEEDbody fusion (33) was used as a potential competitor. Overall, eight VHH SEEDbodies showed competition with B7-H6 for NKp30 binding, indicating that these molecules share the same epitope bin with the natural ligand (Supplemental Fig. 1, Table I). One partially competing molecule was identified (VHH4 SEEDbody) as well as seven noncompeting moieties. Supplemental Fig. 1 shows representative biolayer interferometry sensorgrams for a B7-H6 competitor (VHH1 SEEDbody), a noncompetitor (VHH2 SEEDbody), as well as the partial competitor VHH4 SEEDbody. Moreover, to scrutinize epitope coverage more meticulously, pairwise competition was performed using all VHH SEEDbodies in every possible combination. These experiments revealed that all B7-H6 competing VHH SEEDbodies prevented binding of each other and, therefore, share very similar epitopes on NKp30 (Supplemental Fig. 1, Table I). Additionally, most of them share an overlapping epitope with VHH4 SEEDbody, which partially competes with B7-H6 binding to NKp30. However, VHH12 and VHH15 SEEDbodies did not compete for binding with the VHH4 SEEDbody, indicating also subtle differences of epitope targeting within this set of B7-H6 competitors. Among the B7-H6 noncompeting NKCEs, SEEDbodies harboring VHH8, VHH9, VHH10, and VHH11 share the same epitope bin that partially overlaps with the bins of VHH2 and VHH6 SEEDbodies. Moreover, VHH2, VHH6, and VHH7 SEEDbodies were unique with respect to epitope targeting. In conclusion, the engineered VHH SEEDbodies display a broad epitope diversity represented by seven epitope bins (Supplemental Fig. 1, Table I).

The VHH binding epitope on NKp30 impacts the potency of EGFR × NKp30 NKCEs

Initial functional analyses of the NK cell–engaging VHH SEEDbodies eff− were performed with EGFR-expressing tumor cell lines A431 and A549 using MNCs of healthy donors as effector cells in standard chromium-release assays. Interestingly, the B7-H6 competitors and noncompetitors clustered in two groups, with the B7-H6 competing VHH SEEDbodies eff− mediating more efficient lysis of A431 cells with high EGFR expression levels and A549 cells expressing lower EGFR levels, respectively (Fig. 2A). VHH6 SEEDbody eff−, having the lowest affinity for NKp30 (292 nM) and not interfering with the binding site of the natural ligand B7-H6, elicited the weakest killing of A431 cells in terms of potencies and mediated only negligible lysis of A549 tumor cells (Fig. 2A). This is in contrast to all eight VHH SEEDbodies eff− that compete with the B7-H6 natural ligand binding site on NKp30. These molecules, which exclusively trigger NKp30, induced potent killing similar to monoclonal IgG1 Ab cetuximab, which activates NK cells through FcγRIIIa. This finding was irrespective of higher or lower EGFR expression levels on the tumor cells (Fig. 2A). Based on these results, the three most potent B7-H6 competing NKCEs (VHH1, VHH5, VHH16 SEEDbodies eff−) as well as the three most efficient noncompeting NKCEs (VHH2, VHH4, and VHH8 SEEDbodies eff−) were chosen for further characterization, including VHH4 SEEDbody eff− as a partial competitor. To this end, tumor cell killing assays with A431 and A549 cells using freshly isolated NK cells were performed (Fig. 2B). Ultimately, B7-H6 competitors were more potent than B7-H6 noncompetitors with respect to tumor cell killing, particularly when using tumor cell line A549 with low EGFR expression level, clearly confirming dependencies in killing capacities of VHH-based NKCEs based on the targeted epitope on NKp30.

To address the impact of the EGFR expression level on NK cell–mediated lysis in more detail, three additional cell lines with significantly lower expression levels compared with A431 (epidermoid carcinoma) and A549 (non–small cell lung cancer [NSCLC]) were analyzed (42) for VHH1 and VHH2 SEEDbodies eff− killing, representing the most potent B7-H6 competitor and noncompetitor, respectively. The colorectal cancer cell lines HCT-116 and SW-480 as well as the NSCLC cell line H2030 express significantly lower numbers of EGFR but were efficiently eradicated by our novel NKCEs (Fig. 3). Interestingly, there was no clear correlation between EGFR expression level and maximum lysis of target cells, suggesting that expression levels >50,000 molecules per cell are sufficient for efficient elimination by NK cells. Because the cell lines used in our study have been established from various tumor entities, these data may suggest that the novel NKCEs may represent versatile agents in various indications. Remarkably, the cell lines analyzed harbor different KRAS mutations. Whereas A431 displays a wild-type KRAS status, the other cell lines (A549, HCT-116, SW-480, H2030) harbor homozygous or heterozygous KRAS mutations. Because all cell lines were significantly lysed by NK cells, the KRAS status does not seem to have a

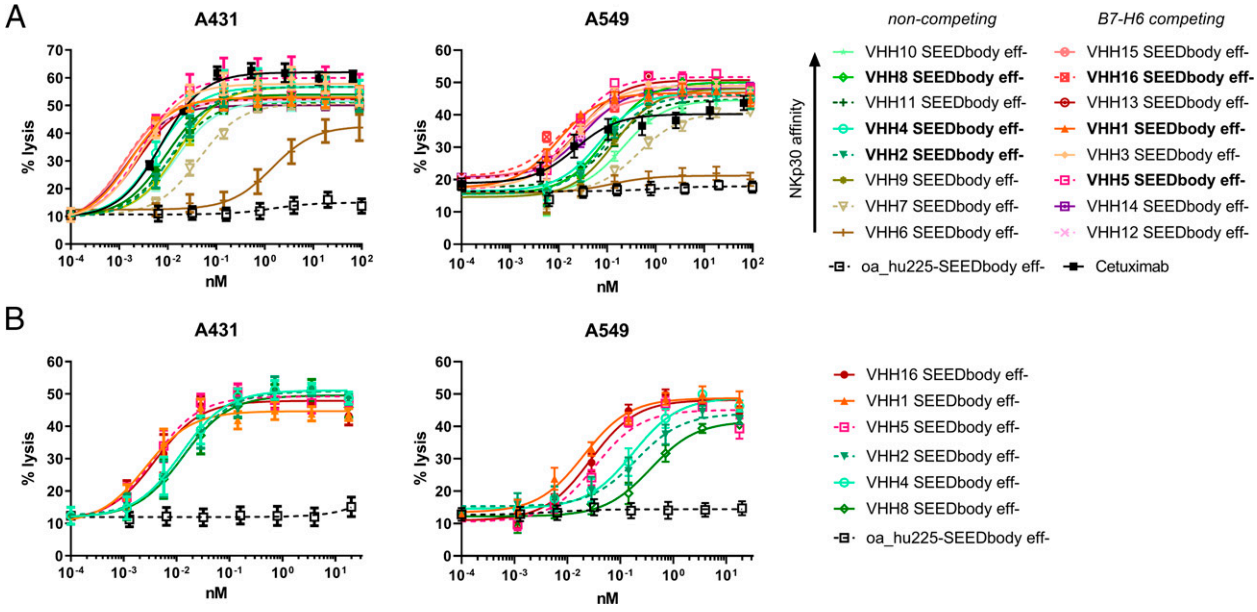

FIGURE 2. EGFR-positive tumor cells are potently lysed by Fc-silenced EGFR × NKp30 VHH SEEDbodies. (**A**) Standard chromium-release assays were performed with high EGFR-expressing A431 cells (left graph) and lower EGFR-expressing A549 cells (right graph) using MNCs of healthy donors at an E:T ratio of 40:1 and increasing concentrations of B7-H6 competing (red colors) and noncompeting VHH SEEDbodies all harboring a humanized version of the Fab fragment of cetuximab (green/brown colors), which activate NK cells only via NKp30. Of note, VHH4 SEEDbody, as a partial competitor, has been included in the panel of noncompeting VHH SEEDbodies. A one-armed SEEDbody lacking the NKp30-activating VHH single-domain Ab (oa_hu225-SEEDbody eff−) and the mAb cetuximab, which activates NK cells solely by FcγRIIIa engagement, were used as controls and for comparison. Mean values ± SEM of three independent experiments with triplicates are shown. Leading candidates for further analyses are depicted in bold. (**B**) B7-H6 competing EGFR × NKp30 VHH SEEDbodies eff− show improved NK cell–mediated lysis of tumor cells compared with noncompeting VHH SEEDbodies eff−. Standard chromium release assays were performed with A431 cells (left graph) and A549 cells (right graph) using isolated NK cells of healthy donors at an E:T ratio of 10:1 and increasing concentrations of B7-H6 competing (red colors) and noncompeting VHH SEEDbodies (green colors) activating NK cells only via NKp30. Of note, VHH4 SEEDbody, as a partial competitor, has been included to the panel of noncompeting VHH SEEDbodies. One-armed SEEDbody lacking the NKp30 activating VHH single-domain Ab (oa_hu225-SEEDbody eff−) was used as a control. Mean values ± SEM of three independent experiments with triplicates are shown.

substantial impact on NK cell–mediated lysis triggered by the NKCEs described in this study (Fig. 3).

We also aimed at assessing whether the generated NKCEs triggering NKp30 are capable of activating CD56^{bright} NK cells, which are generally considered as an important NK cell subset displaying a different phenotype compared with CD56^{dim} NK cells (43). To this end, NK cells were isolated from healthy donors and coincubated with A431 cells in the presence of both VHH SEEDbody-based NKCEs at saturating conditions for 24 h. Afterwards, cells were gated for CD56^{bright} and CD16$^{-/low}$ and stained for CD107a expression as a degranulation marker (Supplemental Fig. 2). Under these experimental conditions, our data suggest that indeed NKCEs triggered the degranulation of this NK cell subset. Importantly, however, it should be noted that isolated NK cells were rested in low-dose IL-2 overnight after isolation, and it is known that this impacts the phenotype (43, 44). Additionally, we observed differences in frequencies of the

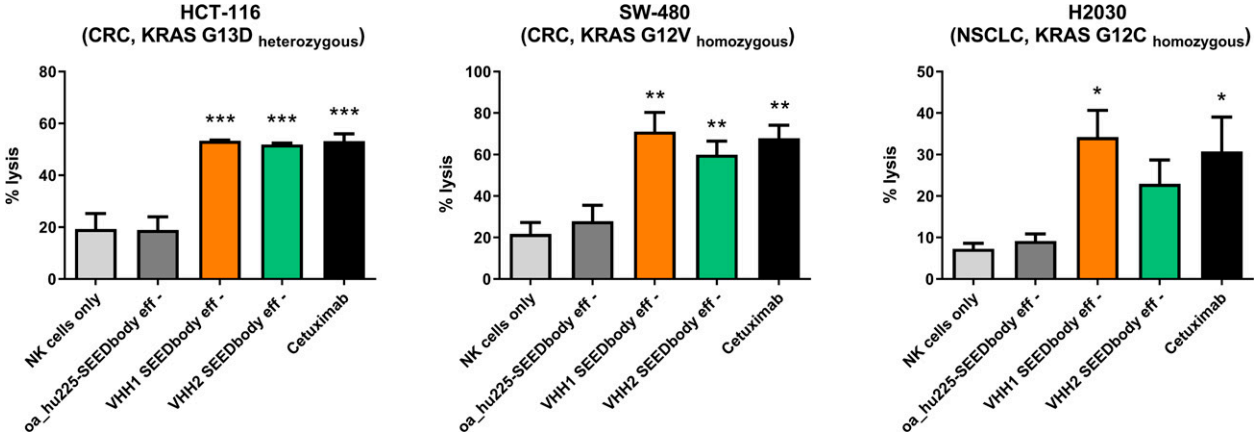

FIGURE 3. Novel EGFR × NKp30 NKCEs are capable of eradicating EGFR-expressing tumor cells from different cancer origins and with different mutations in the EGFR signaling pathway. B7-H6 competing (orange colors) and noncompeting VHH SEEDbodies (green colors) were used at 400 ng/ml with EGRF-positive colorectal cancer (CRC) cell lines HCT-116 (left graph) and SW-480 (middle) as well as non–small cell lung cancer (NSCLC) cell line H2030 (right graph) in standard chromium-release assays with NK cells from healthy donors at an E:T ratio of 10:1. NK cells only (light gray), one-armed SEEDbody lacking the NKp30 activating VHH single-domain Ab (oa_hu225-SEEDbody eff−, dark gray), and cetuximab (black) served as controls. Graphs show mean % lysis ± SEM of three independent experiments. *$p < 0.05$, **$p < 0.01$, ***$p < 0.001$ versus NK cells only.

$CD56^{bright}$ and $CD16^{-/low}$ populations from the same donor after treatment with different molecules (Supplemental Fig. 2).

It is well described that cetuximab blocks the interaction of EGFR and its ligand, thereby inhibiting downstream signaling (45, 46). Importantly, this is often correlated with dermatologic toxicities (47, 48). Because the NKCEs generated in this study harbor the Fab arm derived from a humanized version of cetuximab in a monovalent fashion, we assessed the potential of these molecules to inhibit EGFR downstream signaling by employing the tumor cell line A549. Cetuximab potently inhibited AKT phosphorylation with an EC_{50} of ~0.5 nM (Supplemental Fig. 3). In contrast to this, both analyzed EGFR × NKp30 NKCEs incorporating a monovalent Fab version of humanized cetuximab displayed significantly reduced inhibition capacities, similar to the monovalent EGFR-targeting control (oa_hu225 SEEDbody eff−, EC_{50} of 154.9 nM).

The functional activity of EGFR × NKp30 NKCEs is not negatively impacted by soluble B7-H6

Soluble B7-H6 is found in the serum of cancer patients and could potentially diminish the killing capacities of VHH SEEDbodies that compete for binding to NKp30 with B7-H6 (49). Hence, we performed killing assays with the B7-H6 competing VHH1 SEEDbody

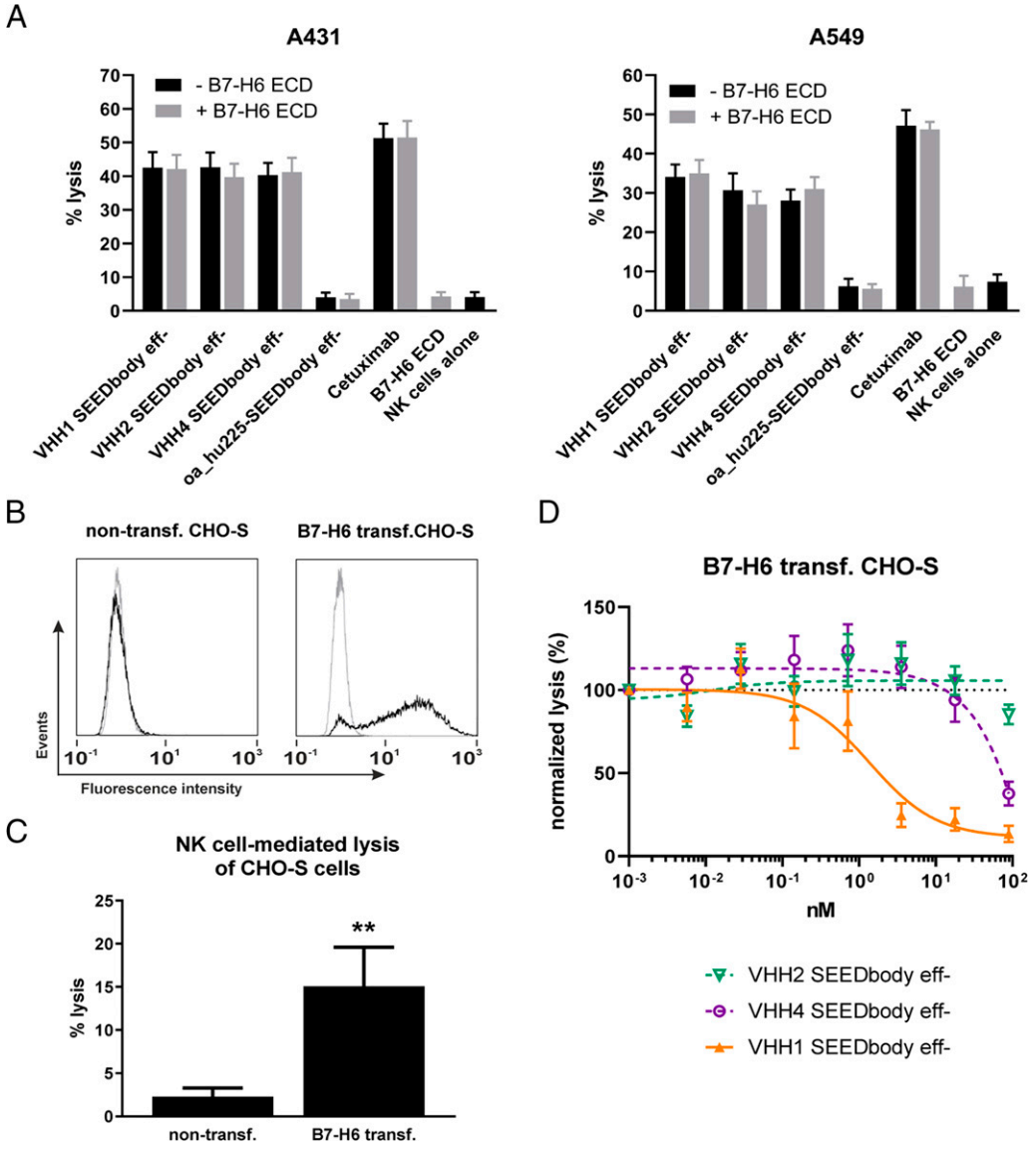

FIGURE 4. Killing of EGFR-positive tumor cells with EGFR × NKp30 VHH SEEDbodies is not impaired by high concentrations of soluble B7-H6, and noncompeting VHH SEEDbodies do not hinder natural elimination of B7-H6–expressing, EGFR-negative cells through NK cells. (**A**) Standard chromium-release assays were performed with A431 (left graph) and A549 cells (right graph) using NK cells of healthy donors at an E:T ratio of 10:1 and saturating concentrations of the B7-H6 competing VHH1, the noncompeting VHH2, or the partially competing VHH4 Fc-silenced SEEDbodies in the presence (gray bars) or absence (black bars) of B7-H6 ECD. The one-armed SEEDbody lacking the NKp30 VHH single-domain Ab (oa_hu225-SEEDbody eff−), the mAb cetuximab, and B7-H6 ECD alone served as controls. Mean values ± SEM of four independent experiments are shown. To analyze whether NK cell–mediated killing by NKp30 and membrane-bound B7-H6 interaction is influenced by VHH SEEDbodies in the absence of a tumor-associated Ag, as a model system CHO-S cells were transiently transfected with human B7-H6. (**B**) Flow cytometry analyses of CHO-S cells 48 h after transfection revealed high B7-H6 expression detected by an anti-human B7-H6 Ab (black) on transfected cells. Staining with secondary Ab alone is shown in gray. (**C**) Using B7-H6 transfected cells as targets together with NK cells in standard ^{51}Cr-release assays significantly enhanced lysis of CHO-S cells. Bars show mean values ± SEM of four independent experiments. $^{**}p \leq 0.01$. (**D**) Lysis of B7-H6–expressing CHO-S cells was not impacted in the presence of the noncompeting VHH2 SEEDbody eff− (green), but it was concentration-dependently impaired by the B7-H6 competing VHH1 (yellow) and the partially competing VHH4 (purple) NKCEs. Percentage of lysis was normalized by using basal release as 0% and % NK cell–mediated lysis without VHH SEEDbody as 100%. Mean values ± SEM of seven independent experiments are shown.

eff−, the partially competing VHH4 SEEDbody eff−, and the noncompeting VHH2 SEEDbody eff− in the presence or absence of high concentrations (178.6 nM) of the B7-H6 ECD (Fig. 4A). Of note, the selected B7-H6 concentration of 178.6 nM was substantially higher than the soluble B7-H6 (sB7-H6) concentration of 5 nM typically found in sera of cancer patients (49). Interestingly, killing of A431 or A549 cells through any of the three NKp30-engaging VHH SEEDbodies was not affected by the B7-H6 ECD, indicating that shed B7-H6 in cancer patients' serum most likely would not directly impair tumor cell killing mediated by the EGFR × NKp30 NKCEs described in this study.

Because NKp30 and B7-H6 are also involved in the crosstalk of NK cells with other types of immune cells and in a variety of physiological processes (2, 50), high-affinity NKp30 binders such as the NKCEs engineered in this study may interfere with this natural axis. To investigate potential effects of our EGFR × NKp30 NKCEs on NK cell killing of EGFR-negative cells expressing the natural ligand B7-H6 as a membrane-bound protein, we transiently transfected CHO-S cells with human B7-H6 as a model system and assessed them together with NK cells in chromium-release assays (Fig. 4B). Of note, NK cell killing of B7-H6–transfected CHO-S cells was significantly enhanced compared with nontransfected cells due to B7-H6–induced activation of NKp30 on NK cells (Fig. 4C). Lysis of B7-H6–expressing CHO-S cells was impaired in the presence of increasing concentrations of the NKCE harboring the B7-H6 competing VHH1, whereas lysis mediated by the NKCE incorporating B7-H6 noncompeting VHH2 was almost unaffected (Fig. 4D). Interestingly, also the NKCE based on B7-H6 partially competing VHH4 did not substantially impede NK cell–mediated killing of B7-H6 displaying CHO-S cells at low concentrations, suggesting that also this sdAb does not interfere with the physiological B7-H6/NKp30 axis.

Coengagement of NKp30 and FcγRIIIa further improves VHH SEEDbody–induced NK cell–mediated tumor cell killing

In an attempt to further enhance the cytotoxic potential of NKCEs generated in this study, we produced NKp30-binding VHH SEEDbodies with an Fc domain capable of binding to FcγRIIIa (VHH SEEDbody eff+) as well. As shown in the upper panel of Fig. 5A, lysis of A431 tumor cells with a high EGFR expression level mediated by B7-H6 competing VHH1 SEEDbody could only be improved with respect to maximal lysis by concomitant engagement of FcγRIIIa, whereas killing potency remained largely unaffected (EC_{50} VHH1 SEEDbody eff− of 2.2 pM versus EC_{50} VHH1 SEEDbody eff+ of 3.2 pM). In contrast, the potency of B7-H6 noncompeting VHH2 SEEDbody was significantly increased by 8.8-fold through the incorporation of an effector functional Fc in the NKCE (EC_{50} VHH2 SEEDbody eff− of 34.4 pM versus EC_{50} VHH2 SEEDbody eff+ of 3.9 pM), whereas no significant differences were observed in maximum lysis rates achieved by both VHH2 SEEDbodies. The VHH4-based constructs partially competing with the B7-H6–binding epitope on NKp30 showed similar characteristics as the VHH2-based SEEDbodies (EC_{50} VHH4 SEEDbody eff− of 36.6 pM versus EC_{50} VHH4 SEEDbody eff+ of 5.1 pM; 7.2-fold more potent) with the exception that also significant differences in maximum killing were observed as for the VHH1 SEEDbodies. In comparison with the clinically approved Ab cetuximab (EC_{50} of 7.7 pM), NKCEs harboring a functional Fc demonstrated similar potency and efficacy in NK cell–mediated A431 tumor cell killing (Fig. 5A). Importantly, when A549 target cells with lower EGFR expression levels were used in a similar experimental setting, the VHH SEEDbodies concomitantly engaging FcγRIIIa and NKp30 clearly outperformed cetuximab in both potencies and efficacies (Fig. 5A, lower panel). Regarding the B7-H6 competing VHH1 SEEDbodies, half-maximal killing of VHH1 SEEDbody eff+ (EC_{50} of 8.7 pM) was 2-fold improved compared with VHH1 SEEDbody eff− (EC_{50} of 16.7 pM), but 14-fold enhanced compared with cetuximab (EC_{50} of 120.9 pM). Even more pronounced were the effects observed with B7-H6 noncompeting VHH2 and partially competing VHH4 SEEDbodies. Both NKCEs harboring an effector-functional Fc achieved a 2.2-fold (EC_{50} VHH2 SEEDbody eff+ of 53.8 pM) and 3.9-fold (EC_{50} VHH4 SEEDbody eff+ of 31.0 pM) improvement in potencies and also substantially enhanced maximum lysis of A549 tumor cells compared with cetuximab. Besides similar killing of cell line A431, both effector-functional SEEDbodies were more potent than their Fc-silenced counterparts with a 5.6-fold (EC_{50} VHH2 SEEDbody eff− of 305.1 pM versus EC_{50} VHH2 SEEDbody eff+ of 53.8 pM) and a 7.2-fold (EC_{50} VHH4 SEEDbody eff− of 223.1 pM versus EC_{50} VHH4 SEEDbody eff+ of 31.0 pM) augmentation in A549 killing. Likewise, significantly enhanced A549 maximum lysis rates were observed for both VHH2- and VHH4-based Fc-effector functional NKCEs (Fig. 5A). These data indicate that coengagement of FcγRIIIa and NKp30 may especially be beneficial when tumor cells express lower target Ag densities. Furthermore, this advantageous effect contributing to overall enhanced antitumor activities seems to be more pronounced for B7-H6 noncompeting or partially competing NKCEs that were not as potent as B7-H6 competing NKCEs in an immune effector-silenced Fc backbone in terms of tumor cell killing.

An important question we also wanted to address was whether strong activation of NK cells mediated by VHH1 SEEDbody might result in activation-induced cell death. Activation-induced NK cell death upon triggering of FcγRIIIa typically occurs within 12 h after NK cell activation (51). Additionally, coengagement of NKp30 on one NK cell as well as FcγRIIIa on another NK cell mediated by a single trifunctional NKCE might result in fratricide. To scrutinize both phenomena, we performed killing assays employing A431 cells in which either the NK cells or, as a control, A431 cells were radioactively labeled (Supplemental Fig. 4A). Essentially, we did not observe killing of NK cells to a substantial extent for all molecules tested. Moreover, no significant differences in killing were obtained between VHH1 SEEDbody and VHH2 SEEDbody as well as between molecules harboring an effector-competent Fc region (eff+) or a Fc-silenced backbone (eff−). These results were confirmed by analyzing NK cell killing in a time-relapsed manner for up to 24 h (Supplemental Fig. 4B). In this study, none of the tested NKCEs mediated higher killing of NK cells compared with cetuximab. Additionally, there were subtle differences in NK cell lysis between untreated cells as well as the monovalent and effector-silenced control molecule (oa_hu225-SEEDbody eff−) and individual NKCEs as well as cetuximab. However, no significant differences were obtained between individual NKCEs.

VHH SEEDbody–based NKCEs display a differentiated profile of proinflammatory cytokine release

Finally, we set out to analyze the tumor-targeted NK cell–mediated release of proinflammatory cytokines IFN-γ and TNF-α by the VHH SEEDbodies (Fig. 5B). As expected, the Fc effector-silenced EGFR-specific control molecule did not trigger the release of detectable levels of IFN-γ, and also the release of TNF-α was negligible (8.6 pg/ml). In contrast to this, therapeutically validated Ab cetuximab elicited the release of detectable levels of IFN-γ (76.0 pg/ml) and TNF-α (18.49 pg/ml) under saturating conditions. Intriguingly, there was a clear trend toward higher IFN-γ release mediated by the VHH SEEDbodies in direct comparison with cetuximab (ranging from 215.9 pg/ml for VHH4 SEEDbody eff+ to 262.6 pg/ml for VHH1 SEEDbody eff+), with the vast majority of molecules triggering the release of significantly elevated levels of this cytokine

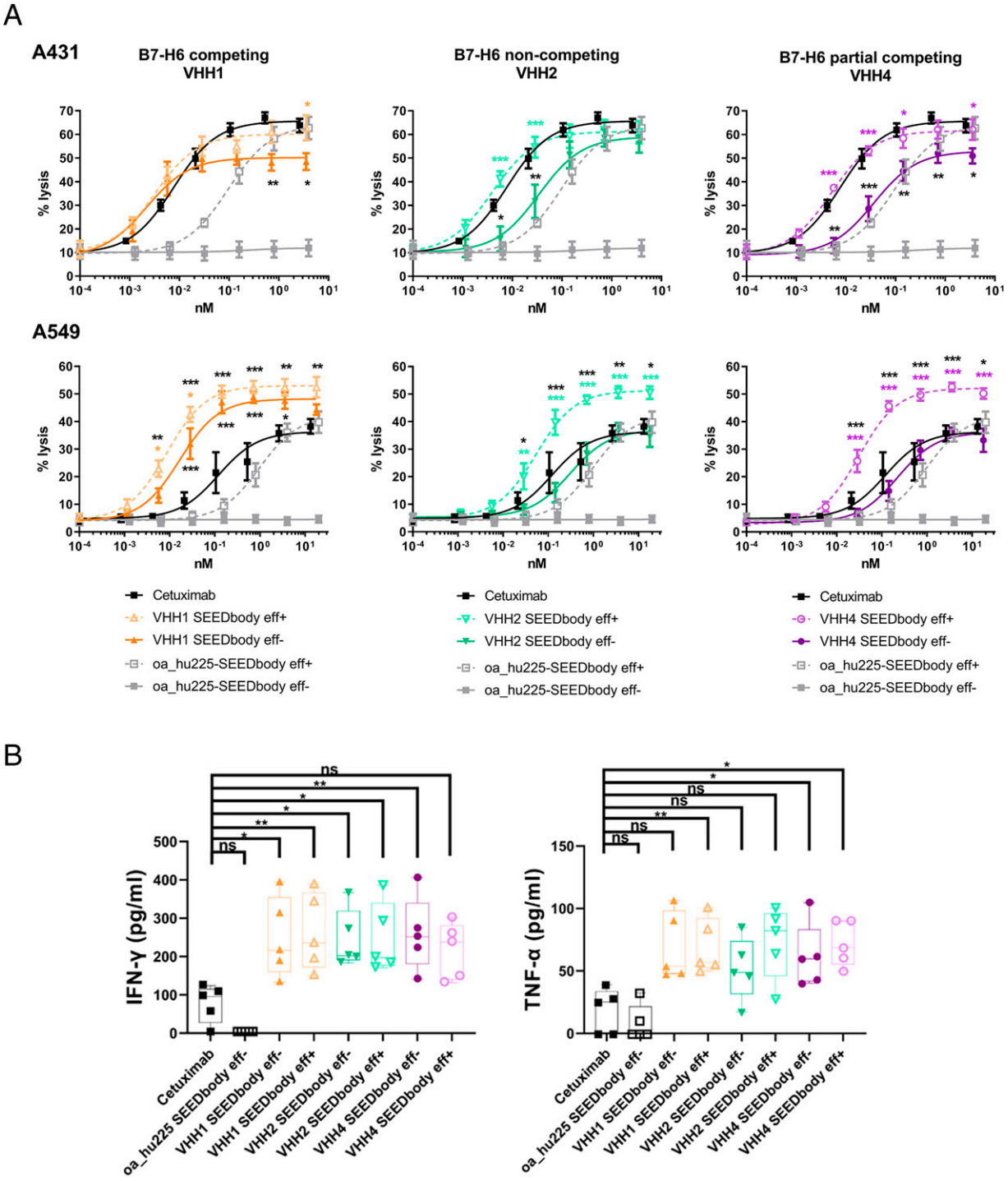

FIGURE 5. Killing of EGFR-positive tumor cells by NKp30 × EGFR NKCEs is further improved by an effector functional Fc. (**A**) Standard chromium-release assays were performed with A431 cells (upper graphs) and A549 cells (lower graphs) using isolated NK cells of healthy donors at an E:T ratio of 10:1 and increasing concentrations of B7-H6 competing VHH1 SEEDbodies (orange colors; left panel), noncompeting VHH2 SEEDbodies (green colors; middle panel), and partially competing VHH4 SEEDbodies (purple colors; right panel) harboring either an effector functional (eff+; continuous lines, filled symbols) or nonfunctional (eff−; dotted lines, open symbols) Fc. One-armed SEEDbodies lacking the NKp30 VHH single domain Ab but carrying the effector functional (oa_hu225-SEEDbody eff+) or nonfunctional (oa_hu225-SEEDbody eff-) Fc as well as the monoclonal IgG1 Ab cetuximab were used as controls and for comparison. Mean values ± SEM of four independent experiments with triplicates are shown. *$p \leq 0.05$, **$p \leq 0.01$, ***$p \leq 0.001$, VHH SEEDbody eff+ compared with respective VHH SEEDbody eff− (colored) or VHH SEEDbody versus cetuximab (black). (**B**) NKp30 × EGFR NKCEs display a differentiated cytokine-release profile compared with therapeutic Ab cetuximab. NKCEs were compared with cetuximab with respect to promoting NK cell–mediated IFN-γ and TNF-α release using cytokine HTRF kits for quantification. Purified NK cells were cocultured with A431 cells for 24 h at an E:T ratio of 5:1 prior to analysis. Graphs show box-and-whisker plots as superimposition with dot plots of seven individual experiments. *$p \leq 0.05$, ** $p \leq 0.01$. n.s., not significant (compared with cetuximab).

(Fig. 5B). Moreover, the engineered molecules did not behave appreciably different depending on the type of Fc that had been incorporated, that is, Fc effector-competent backbone versus immune effector-silenced Fc part. Importantly, we also observed this trend of elevated cytokine release for the proinflammatory molecule TNF-α. Although not as pronounced as ascertained for IFN-γ,

VHH SEEDbodies promoted NK cell–mediated release of TNF-α in a tumor cell–targeted fashion in the range of 51.9 pg/ml (VHH2 SEEDbody eff−) to 71.9 pg/ml (VHH4 SEEDbody eff+), clearly indicating a distinguished cytokine release profile compared with cetuximab.

Discussion

To redirect NK cell cytotoxicity against EGFR-expressing tumor cells by triggering NKp30, we generated a panel of EGFR × NKp30 NKCEs based on novel VHH sdAbs binding to different epitopes on the NKp30 receptor. For this, we combined camelid immunization with yeast surface display (38, 52). We focused on camelid single-domain paratopes, because it is well known that these molecules display several beneficial attributes such as their ease of generation or multiple reformatting options, rendering VHHs as promising moieties for therapeutic applications (53–58). Indeed, with caplacizumab, one VHH-based therapeutic has already been granted marketing approval for the treatment of thrombotic thrombocytopenic purpura (59–61). After Ab hit discovery and reformatting into EGFR-targeting NKCEs, these novel agents triggered significant lysis of tumor cells by engaging NK cells and promoted robust release of proinflammatory cytokines TNF-α and IFN-γ.

Therapeutic interventions based on NK cells represent interesting approaches to further improve therapy of malignant diseases (2, 5, 62). NK cell activation is regulated by a complex interplay of activating and inhibitory receptors (63, 64), and either blocking inhibitory NK cell receptors (65) or triggering stimulatory receptors such as NKp30, NKp46, NKG2D or FcγRIIIa (25, 27, 28, 32, 66) may be suitable for therapeutic intervention. Tumor cells escape elimination by NK cells by preventing surface exposure or shedding of stress-induced ligands, for example B7-H6, for activating NK cell receptors such as NKp30 (9–11, 67). Therefore, different Ab-based approaches targeting various activating NK cell receptors have been pursued to restore recognition of tumor cells by NK cells (7, 27, 33, 68). Earlier studies demonstrated that tumor cell killing by NK cells could be significantly enhanced by fusing the ECDs of natural ligands for activating NK cell receptors to Abs or Ab fragments (31, 32, 69). In a recent study, we were able to demonstrate that B7-H6–based immunoligands, in which affinity maturated B7-H6 variants were used, efficiently activated NK cells and potently triggered tumor cell lysis (33). Although these types of NKCEs based on natural ligands directed against activating NK cell receptors may represent promising agents in cancer immunotherapy, alternative NKCEs such as the Ab-based NKCEs may have favorable characteristics that distinguish these molecules from immunoligands (70). Molecules such as B7-H6 or AICL used for the generation of immunoligands are highly glycosylated and the glycosylation status may impact their functional activity (31). Moreover, glycosylation might cause product heterogeneity and thus could hamper developability of such molecules (71, 72). Hence, replacing the natural ligands by VHH Abs may be advantageous. Beyond these more technical issues, using VHH sdAbs targeting a more diverse set of epitopes on NKp30 offers novel opportunities for therapeutic intervention. Besides modulating NK cell cytotoxicity, the B7-H6/NKp30 axis has been demonstrated to modulate crosstalk between NK cells and other cell types of the immune system (2, 50) and has been suggested to modulate the interaction of group 2 innate lymphoid cells and monocytic myeloid-derived suppressor cells (73). Therefore, B7-H6–based immunoligands may interfere with different physiological and pathophysiological processes, which might be warranted or unwanted, depending on the respective setting or application. With the set of EGFR × NKp30 NKCEs including B7-H6 competitors and noncompetitors engineered in this study, we developed a toolkit allowing either triggering NK cell cytotoxicity without disturbing B7-H6/NKp30 interactions or to block this axis. The pros and cons of each approach have to be elucidated in the future via in vivo studies.

Interestingly, the binding epitope of the NKp30-specific VHH (B7-H6–blocking versus noncompeting VHH) had a significant impact on the capacity of NKCEs to trigger NK cell cytotoxicity against EGFR-positive tumor cells. The most active molecules were derived from the group of B7-H6 competing VHH sdAbs. Nevertheless, potent EGFR × NKp30 NKCEs were also derived from the group of B7-H6 noncompeting VHH sdAbs, indicating that strong NK cell activation via NKp30 does not solely rely on targeting the actual natural ligand binding site on NKp30 (74, 75). High-affinity NKp30 binding seemed not to be the most important determinant for NK cell activation, because especially in the noncompeting group, VHH8 SEEDbody displaying the highest affinity for NKp30 was not as efficient in terms of killing A549 target cells with isolated NK cells as noncompeting NKCEs with lower binding affinities. However, our data suggest that binding affinity impacts the biological function of the generated NKCEs to some extent. B7-H6 noncompeting VHH6 SEEDbody displaying low-affinity binding to NKp30 in the triple nanomolar range was overall the least competent molecule in this study in terms of killing EGFR-positive tumor cells. This is in line with previous findings for other Abs, for which it has been shown that affinity beyond a certain threshold may not necessarily result in improved cytolytic activity and may even be detrimental (76–78).

Of note, the leading candidates of generated EGFR × NKp30 NKCEs achieved picomolar EC_{50} values irrespective of EGFR expression levels and regardless of the NKp30 binding epitope (i.e., B7-H6 competition). Concomitant engagement of NKp30 and FcγRIIIa by implementing an effector-competent Fc domain resulted in further enhanced half-maximal killing by up to 8.8-fold and a significant increase in maximal tumor cell lysis rates for most of these novel molecules. This improvement was more pronounced with EGFR × NKp30 NKCEs carrying an NKp30-specific VHH not competing with the B7-H6 natural ligand binding site. Interestingly, the NKCEs triggering FcγRIIIa and NKp30 on NK cells demonstrated an up to 3.9-fold increased efficacy and >10% higher maximum tumor cell lysis compared with cetuximab with tumor cells having lower EGFR density. These findings are in line with a recent report demonstrating that concomitant engagement of FcγRIIIa and NKp46 significantly enhances cytotoxicity and in vivo activity of engineered Ab derivatives (27). Furthermore, neither tumor cell killing of B7-H6 competing or noncompeting NKCEs was impaired by soluble B7-H6 at concentrations much higher than shed B7-H6 levels found in cancer patients (49). In addition, the novel NKCEs promoted a robust release of proinflammatory cytokines TNF-α and INF-γ, with most of the molecules being significantly more efficacious compared with therapeutic Ab cetuximab. This result was irrespective of whether the NKCE harbored an Fc domain capable in FcγR binding. These findings are in line with our previous findings with engineered B7-H6 immunoligands and further underline that triggering the FcγRIIIa in parallel to NKp30 has no inhibitory effect on cytokine release (33). The capacity to trigger augmented production of proinflammatory cytokines may have an important impact when used in vivo. For example, IFN-γ acts on various immune cell types in the tumor microenvironment (79–82). On the one hand, IFN-γ may enhance tumor elimination by inhibiting myeloid-derived suppressor cells, tumor-associated macrophages, as well as regulatory T cells (83); on the other hand, IFN-γ may promote trafficking of NK, NKT, and T cells into solid tumors (84, 85). Because IFN-γ also stimulates APCs and cytotoxic T lymphocytes, the engineered EGFR × NKp30 NKCEs may be promising combination

partners for therapeutic compounds with immunomodulatory function (e.g., immune checkpoint inhibitors or immunomodulatory drugs) (86, 87). In this study, we exploited a monovalent EGFR-targeting arm derived from a humanized version of cetuximab for the construction of NKCEs. For cetuximab it is well established that part of the clinical benefit, but also the skin toxicities associated with therapy, can be attributed to the inhibition of EGFR signaling (46–48). Importantly, monovalent targeting of EGFR reduced EGFR-mediated AKT phosphorylation by a factor of ~300. Hence, it might be envisioned that the NKCEs engineered in this study might display a better safety profile compared with cetuximab, but ultimately, this could only be analyzed in clinical trials.

In conclusion, the EGFR × NKp30 NKCEs generated in this study may represent interesting NK cell–activating and immunomodulatory agents for cancer immunotherapy that may promote a complex and sophisticated antitumoral immune response.

Acknowledgments

We thank Britta von Below and Anja Muskulus for excellent technical assistance. Moreover, we are grateful to Kerstin Hallstein, Laura Unmuth, Stephan Keller, Alexander Mueller, Sigrid Auth, Pia Stroh, Marion Wetter, Thomas Rysiok, Janina Klemm, Hanbyul Yoo, Stefan Becker, and Dirk Mueller-Pompalla for experimental support.

Disclosures

L.P., S.K., L.T., and S.Z. filed a patent application based on this work. In addition, L.P., T.G., Y.X., S.K., R.Z., L.T., S.P., B.R., and S.Z. are or were employees either at Merck Healthcare KGaA or EMD Serono. The other authors have no conflicts of interest.

References

1. Carlsten, M., and M. Järås. 2019. Natural killer cells in myeloid malignancies: immune surveillance, NK cell dysfunction, and pharmacological opportunities to bolster the endogenous NK cells. *Front. Immunol.* 10: 2357.
2. Huntington, N. D., J. Cursons, and J. Rautela. 2020. The cancer-natural killer cell immunity cycle. *Nat. Rev. Cancer* 20: 437–454.
3. Gonzalez-Rodriguez, A. P., M. Villa-Álvarez, C. Sordo-Bahamonde, S. Lorenzo-Herrero, and S. Gonzalez. 2019. NK cells in the treatment of hematological malignancies. *J. Clin. Med.* 8: 1557.
4. Kiessling, R., E. Klein, H. Pross, and H. Wigzell. 1975. "Natural" killer cells in the mouse. II. Cytotoxic cells with specificity for mouse Moloney leukemia cells. Characteristics of the killer cell. *Eur. J. Immunol.* 5: 117–121.
5. Chiossone, L., P.-Y. Dumas, M. Vienne, and E. Vivier. 2018. Natural killer cells and other innate lymphoid cells in cancer. [Published erratum appears in 2018 *Nat. Rev. Immunol.* 18: 726.] *Nat. Rev. Immunol.* 18: 671–688.
6. Vivier, E., E. Tomasello, M. Baratin, T. Walzer, and S. Ugolini. 2008. Functions of natural killer cells. *Nat. Immunol.* 9: 503–510.
7. Koch, J., and M. Tesar. 2017. Recombinant antibodies to arm cytotoxic lymphocytes in cancer immunotherapy. *Transfus. Med. Hemother.* 44: 337–350.
8. Morgado, S., B. Sanchez-Correa, J. G. Casado, E. Duran, I. Gayoso, F. Labella, R. Solana, and R. Tarazona. 2011. NK cell recognition and killing of melanoma cells is controlled by multiple activating receptor-ligand interactions. *J. Innate Immun.* 3: 365–373.
9. Reiners, K. S., D. Topolar, A. Henke, V. R. Simhadri, J. Kessler, M. Sauer, M. Bessler, H. P. Hansen, S. Tawadros, M. Herling, et al. 2013. Soluble ligands for NK cell receptors promote evasion of chronic lymphocytic leukemia cells from NK cell anti-tumor activity. *Blood* 121: 3658–3665.
10. Wang, W., H. Guo, J. Geng, X. Zheng, H. Wei, R. Sun, and Z. Tian. 2014. Tumor-released Galectin-3, a soluble inhibitory ligand of human NKp30, plays an important role in tumor escape from NK cell attack. *J. Biol. Chem.* 289: 33311–33319.
11. Schlecker, E., N. Fiegler, A. Arnold, P. Altevogt, S. Rose-John, G. Moldenhauer, A. Sucker, A. Paschen, E. P. von Strandmann, S. Textor, and A. Cerwenka. 2014. Metalloprotease-mediated tumor cell shedding of B7-H6, the ligand of the natural killer cell-activating receptor NKp30. *Cancer Res.* 74: 3429–3440.
12. Balsamo, M., W. Vermi, M. Parodi, G. Pietra, C. Manzini, P. Queirolo, S. Lonardi, R. Augugliaro, A. Moretta, F. Facchetti, et al. 2012. Melanoma cells become resistant to NK-cell-mediated killing when exposed to NK-cell numbers compatible with NK-cell infiltration in the tumor. *Eur. J. Immunol.* 42: 1833–1842.
13. Bryceson, Y. T., M. E. March, D. F. Barber, H.-G. Ljunggren, and E. O. Long. 2005. Cytolytic granule polarization and degranulation controlled by different receptors in resting NK cells. *J. Exp. Med.* 202: 1001–1012.
14. Seidel, U. J. E., P. Schlegel, and P. Lang. 2013. Natural killer cell mediated antibody-dependent cellular cytotoxicity in tumor immunotherapy with therapeutic antibodies. *Front. Immunol.* 4: 76.
15. Bibeau, F., E. Lopez-Crapez, F. Di Fiore, S. Thezenas, M. Ychou, F. Blanchard, A. Lamy, F. Penault-Llorca, T. Frébourg, P. Michel, et al. 2009. Impact of FcγRIIa-FcγRIIIa polymorphisms and *KRAS* mutations on the clinical outcome of patients with metastatic colorectal cancer treated with cetuximab plus irinotecan. *J. Clin. Oncol.* 27: 1122–1129.
16. Weng, W.-K., and R. Levy. 2003. Two immunoglobulin G fragment C receptor polymorphisms independently predict response to rituximab in patients with follicular lymphoma. *J. Clin. Oncol.* 21: 3940–3947.
17. Musolino, A., N. Naldi, B. Bortesi, D. Pezzuolo, M. Capelletti, G. Missale, D. Laccabue, A. Zerbini, R. Camisa, G. Bisagni, et al. 2008. Immunoglobulin G fragment C receptor polymorphisms and clinical efficacy of trastuzumab-based therapy in patients with HER-2/*neu*-positive metastatic breast cancer. *J. Clin. Oncol.* 26: 1789–1796.
18. Preithner, S., S. Elm, S. Lippold, M. Locher, A. Wolf, A. J. da Silva, P. A. Baeuerle, and N. S. Prang. 2006. High concentrations of therapeutic IgG1 antibodies are needed to compensate for inhibition of antibody-dependent cellular cytotoxicity by excess endogenous immunoglobulin G. *Mol. Immunol.* 43: 1183–1193.
19. Grzywacz, B., N. Kataria, and M. R. Verneris. 2007. $CD56^{dim}CD16^{+}$ NK cells downregulate CD16 following target cell induced activation of matrix metalloproteinases. *Leukemia* 21: 356–359, author reply 359.
20. Carrega, P., B. Morandi, R. Costa, G. Frumento, G. Forte, G. Altavilla, G. B. Ratto, M. C. Mingari, L. Moretta, and G. Ferlazzo. 2008. Natural killer cells infiltrating human nonsmall-cell lung cancer are enriched in $CD56^{bright}$ $CD16^{-}$ cells and display an impaired capability to kill tumor cells. *Cancer* 112: 863–875.
21. Schleypen, J. S., N. Baur, R. Kammerer, P. J. Nelson, K. Rohrmann, E. F. Gröne, M. Hohenfellner, A. Haferkamp, H. Pohla, D. J. Schendel, et al. 2006. Cytotoxic markers and frequency predict functional capacity of natural killer cells infiltrating renal cell carcinoma. *Clin. Cancer Res.* 12: 718–725.
22. Myers, J. A., and J. S. Miller. 2021. Exploring the NK cell platform for cancer immunotherapy. *Nat. Rev. Clin. Oncol.* 18: 85–100.
23. Minetto, P., F. Guolo, S. Pesce, M. Greppi, V. Obino, E. Ferretti, S. Sivori, C. Genova, R. M. Lemoli, and E. Marcenaro. 2019. Harnessing NK cells for cancer treatment. *Front. Immunol.* 10: 2836.
24. Rothe, A., S. Sasse, M. S. Topp, D. A. Eichenauer, H. Hummel, K. S. Reiners, M. Dietlein, G. Kuhnert, J. Kessler, C. Buerkle, et al. 2015. A phase 1 study of the bispecific anti-CD30/CD16A antibody construct AFM13 in patients with relapsed or refractory Hodgkin lymphoma. *Blood* 125: 4024–4031.
25. Ellwanger, K., U. Reusch, I. Fucek, S. Wingert, T. Ross, T. Müller, U. Schniegler-Mattox, T. Haneke, E. Rajkovic, J. Koch, et al. 2019. Redirected optimized cell killing (ROCK®): a highly versatile multispecific fit-for-purpose antibody platform for engaging innate immunity. *MAbs* 11: 899–918.
26. Rozan, C., A. Cornillon, C. Pétiard, M. Chartier, G. Behar, C. Boix, B. Kerfelec, B. Robert, A. Pèlegrin, P. Chames, et al. 2013. Single-domain antibody-based and linker-free bispecific antibodies targeting FcγRIII induce potent antitumor activity without recruiting regulatory T cells. *Mol. Cancer Ther.* 12: 1481–1491.
27. Gauthier, L., A. Morel, N. Anceriz, B. Rossi, A. Blanchard-Alvarez, G. Grondin, S. Trichard, C. Cesari, M. Sapet, F. Bosco, et al. 2019. Multifunctional natural killer cell engagers targeting NKp46 trigger protective tumor immunity. *Cell* 177: 1701–1713.e16.
28. Raynaud, A., K. Desrumeaux, L. Vidard, E. Termine, D. Baty, P. Chames, E. Vigne, and B. Kerfelec. 2020. Anti-NKG2D single domain-based antibodies for the modulation of anti-tumor immune response. *OncoImmunology* 10: 1854529.
29. Murer, P., and D. Neri. 2019. Antibody-cytokine fusion proteins: a novel class of biopharmaceuticals for the therapy of cancer and of chronic inflammation. *N. Biotechnol.* 52: 42–53.
30. Wang, T., F. Sun, W. Xie, M. Tang, H. He, X. Jia, X. Tian, M. Wang, and J. Zhang. 2016. A bispecific protein rG7S-MICA recruits natural killer cells and enhances NKG2D-mediated immunosurveillance against hepatocellular carcinoma. *Cancer Lett.* 372: 166–178.
31. Peipp, M., S. Derer, S. Lohse, M. Staudinger, K. Klausz, T. Valerius, M. Gramatzki, and C. Kellner. 2015. HER2-specific immunoligands engaging NKp30 or NKp80 trigger NK-cell-mediated lysis of tumor cells and enhance antibody-dependent cell-mediated cytotoxicity. *Oncotarget* 6: 32075–32088.
32. von Strandmann, E. P., H. P. Hansen, K. S. Reiners, R. Schnell, P. Borchmann, S. Merkert, V. R. Simhadri, A. Draube, M. Reiser, I. Purr, et al. 2006. A novel bispecific protein (ULBP2-BB4) targeting the NKG2D receptor on natural killer (NK) cells and CD138 activates NK cells and has potent antitumor activity against human multiple myeloma in vitro and in vivo. *Blood* 107: 1955–1962.
33. Pekar, L., K. Klausz, M. Busch, B. Valldorf, H. Kolmar, D. Wesch, H.-H. Oberg, S. Krohn, A. S. Boje, C. L. Gehlert, et al. 2021. Affinity maturation of B7-H6 translates into enhanced NK cell-mediated tumor cell lysis and improved proinflammatory cytokine release of bispecific immunoligands via NKp30 engagement. *J. Immunol.* 206: 225–236.
34. Pende, D., S. Parolini, A. Pessino, S. Sivori, R. Augugliaro, L. Morelli, E. Marcenaro, L. Accame, A. Malaspina, R. Biassoni, et al. 1999. Identification and molecular characterization of NKp30, a novel triggering receptor involved in natural cytotoxicity mediated by human natural killer cells. *J. Exp. Med.* 190: 1505–1516.
35. Correia, M. P., A. Stojanovic, K. Bauer, D. Juraeva, L.-O. Tykocinski, H.-M. Lorenz, B. Brors, and A. Cerwenka. 2018. Distinct human circulating $NKp30^{+}$ $FcεRIγ^{+}CD8^{+}$ T cell population exhibiting high natural killer-like antitumor potential. *Proc. Natl. Acad. Sci. USA* 115: E5980–E5989.

36. Lawand, M., J. Déchanet-Merville, and M.-C. Dieu-Nosjean. 2017. Key features of gamma-delta T-cell subsets in human diseases and their immunotherapeutic implications. *Front. Immunol.* 8: 761.
37. Roth, L., S. Krah, J. Klemm, R. Günther, L. Toleikis, M. Busch, S. Becker, and S. Zielonka. 2020. Isolation of antigen-specific VHH single-domain antibodies by combining animal immunization with yeast surface display. *Methods Mol. Biol.* 2070: 173–189.
38. Valldorf, B., S. C. Hinz, G. Russo, L. Pekar, L. Mohr, J. Klemm, A. Doerner, S. Krah, M. Hust, and S. Zielonka. 2021. Antibody display technologies: selecting the cream of the crop. *Biol. Chem.* 403: 455–477.
39. Repp, R., C. Kellner, A. Muskulus, M. Staudinger, S. M. Nodehi, P. Glorius, D. Akramiene, M. Dechant, G. H. Fey, P. H. C. van Berkel, et al. 2011. Combined Fc-protein- and Fc-glyco-engineering of scFv-Fc fusion proteins synergistically enhances CD16a binding but does not further enhance NK-cell mediated ADCC. *J. Immunol. Methods* 373: 67–78.
40. Wong, S.-F. 2005. Cetuximab: an epidermal growth factor receptor monoclonal antibody for the treatment of colorectal cancer. *Clin. Ther.* 27: 684–694.
41. Davis, J. H., C. Aperlo, Y. Li, E. Kurosawa, Y. Lan, K.-M. Lo, and J. S. Huston. 2010. SEEDbodies: fusion proteins based on strand-exchange engineered domain (SEED) CH3 heterodimers in an Fc analogue platform for asymmetric binders or immunofusions and bispecific antibodies. *Protein Eng. Des. Sel.* 23: 195–202.
42. Schlaeth, M., S. Berger, S. Derer, K. Klausz, S. Lohse, M. Dechant, G. A. Lazar, T. Schneider-Merck, M. Peipp, and T. Valerius. 2010. Fc-engineered EGF-R antibodies mediate improved antibody-dependent cellular cytotoxicity (ADCC) against *KRAS*-mutated tumor cells. *Cancer Sci.* 101: 1080–1088.
43. Poli, A., T. Michel, M. Thérésine, E. Andrès, F. Hentges, and J. Zimmer. 2009. $CD56^{bright}$ natural killer (NK) cells: an important NK cell subset. *Immunology* 126: 458–465.
44. Ferlazzo, G., D. Thomas, S.-L. Lin, K. Goodman, B. Morandi, W. A. Muller, A. Moretta, and C. Münz. 2004. The abundant NK cells in human secondary lymphoid tissues require activation to express killer cell Ig-like receptors and become cytolytic. *J. Immunol.* 172: 1455–1462.
45. Li, S., K. R. Schmitz, P. D. Jeffrey, J. J. W. Wiltzius, P. Kussie, and K. M. Ferguson. 2005. Structural basis for inhibition of the epidermal growth factor receptor by cetuximab. *Cancer Cell* 7: 301–311.
46. Cai, W.-Q., L.-S. Zeng, L.-F. Wang, Y.-Y. Wang, J.-T. Cheng, Y. Zhang, Z.-W. Han, Y. Zhou, S.-L. Huang, X.-W. Wang, et al. 2020. The latest battles between EGFR monoclonal antibodies and resistant tumor cells. *Front. Oncol.* 10: 1249.
47. Holcmann, M., and M. Sibilia. 2015. Mechanisms underlying skin disorders induced by EGFR inhibitors. *Mol. Cell. Oncol.* 2: e1004969.
48. Li, Y., R. Fu, T. Jiang, D. Duan, Y. Wu, C. Li, Z. Li, R. Ni, L. Li, and Y. Liu. 2022. Mechanism of lethal skin toxicities induced by epidermal growth factor receptor inhibitors and related treatment strategies. *Front. Oncol.* 12: 804212.
49. Rusakiewicz, S., A. Perier, M. Semeraro, J. M. Pitt, E. Pogge von Strandmann, K. S. Reiners, S. Aspeslagh, C. Pipéroglou, F. Vély, A. Ivagnes, et al. 2016. NKp30 isoforms and NKp30 ligands are predictive biomarkers of response to imatinib mesylate in metastatic GIST patients. *OncoImmunology* 6: e1137418.
50. Pesce, S., F. B. Thoren, C. Cantoni, C. Prato, L. Moretta, A. Moretta, and E. Marcenaro. 2017. The innate immune cross talk between NK cells and eosinophils is regulated by the interaction of natural cytotoxicity receptors with eosinophil surface ligands. *Front. Immunol.* 8: 510.
51. Ida, H., and P. Anderson. 1998. Activation-induced NK cell death triggered by CD2 stimulation. *Eur. J. Immunol.* 28: 1292–1300.
52. Doerner, A., L. Rhiel, S. Zielonka, and H. Kolmar. 2014. Therapeutic antibody engineering by high efficiency cell screening. *FEBS Lett.* 588: 278–287.
53. Pekar, L., M. Busch, B. Valldorf, S. C. Hinz, L. Toleikis, S. Krah, and S. Zielonka. 2020. Biophysical and biochemical characterization of a VHH-based IgG-like bi- and trispecific antibody platform. *MAbs* 12: 1812210.
54. Sellmann, C., L. Pekar, C. Bauer, E. Ciesielski, S. Krah, S. Becker, L. Toleikis, J. Kügler, A. Frenzel, B. Valldorf, et al. 2020. A one-step process for the construction of phage display scFv and VHH libraries. *Mol. Biotechnol.* 62: 228–239.
55. Könning, D., S. Zielonka, J. Grzeschik, M. Empting, B. Valldorf, S. Krah, C. Schröter, C. Sellmann, B. Hock, and H. Kolmar. 2017. Camelid and shark single domain antibodies: structural features and therapeutic potential. *Curr. Opin. Struct. Biol.* 45: 10–16.
56. Krah, S., C. Schröter, S. Zielonka, M. Empting, B. Valldorf, and H. Kolmar. 2016. Single-domain antibodies for biomedical applications. *Immunopharmacol. Immunotoxicol.* 38: 21–28.
57. Bannas, P., J. Hambach, and F. Koch-Nolte. 2017. Nanobodies and nanobody-based human heavy chain antibodies as antitumor therapeutics. *Front. Immunol.* 8: 1603.
58. Jovčevska, I., and S. Muyldermans. 2020. The therapeutic potential of nanobodies. *BioDrugs* 34: 11–26.
59. Scully, M., S. R. Cataland, F. Peyvandi, P. Coppo, P. Knöbl, J. A. Kremer Hovinga, A. Metjian, J. de la Rubia, K. Pavenski, F. Callewaert, et al.; HERCULES Investigators. 2019. Caplacizumab treatment for acquired thrombotic thrombocytopenic purpura. *N. Engl. J. Med.* 380: 335–346.
60. Duggan, S. 2018. Caplacizumab: first global approval. [Published erratum appears in 2018 *Drugs* 78: 1955.] *Drugs* 78: 1639–1642.
61. Elverdi, T., and A. E. Eskazan. 2019. Caplacizumab as an emerging treatment option for acquired thrombotic thrombocytopenic purpura. *Drug Des. Devel. Ther.* 13: 1251–1258.
62. Peipp, M., K. Klausz, A. S. Boje, T. Zeller, S. Zielonka, and C. Kellner. 2022. Immunotherapeutic targeting of activating natural killer cell receptors and their ligands in cancer. *Clin. Exp. Immunol.* 209: 22–32.
63. Morvan, M. G., and L. L. Lanier. 2016. NK cells and cancer: you can teach innate cells new tricks. *Nat. Rev. Cancer* 16: 7–19.
64. Shimasaki, N., A. Jain, and D. Campana. 2020. NK cells for cancer immunotherapy. *Nat. Rev. Drug Discov.* 19: 200–218.
65. van Hall, T., P. André, A. Horowitz, D. F. Ruan, L. Borst, R. Zerbib, E. Narni-Mancinelli, S. H. van der Burg, and E. Vivier. 2019. Monalizumab: inhibiting the novel immune checkpoint NKG2A. *J. Immunother. Cancer* 7: 263.
66. Chan, W. K., S. Kang, Y. Youssef, E. N. Glankler, E. R. Barrett, A. M. Carter, E. H. Ahmed, A. Prasad, L. Chen, J. Zhang, et al. 2018. A CS1-NKG2D bispecific antibody collectively activates cytolytic immune cells against multiple myeloma. *Cancer Immunol. Res.* 6: 776–787.
67. Chitadze, G., M. Lettau, J. Bhat, D. Wesch, A. Steinle, D. Fürst, J. Mytilineos, H. Kalthoff, O. Janssen, H.-H. Oberg, and D. Kabelitz. 2013. Shedding of endogenous MHC class I-related chain molecules A and B from different human tumor entities: heterogeneous involvement of the "a disintegrin and metalloproteases" 10 and 17. *Int. J. Cancer* 133: 1557–1566.
68. Vallera, D. A., M. Felices, R. McElmurry, V. McCullar, X. Zhou, J. U. Schmohl, B. Zhang, A. J. Lenvik, A. Panoskaltsis-Mortari, M. R. Verneris, et al. 2016. IL15 trispecific killer engagers (TriKE) make natural killer cells specific to $CD33^{+}$ targets while also inducing persistence, *in vivo* expansion, and enhanced function. *Clin. Cancer Res.* 22: 3440–3450.
69. Kellner, C., A. Günther, A. Humpe, R. Repp, K. Klausz, S. Derer, T. Valerius, M. Ritgen, M. Brüggemann, J. G. van de Winkel, et al. 2015. Enhancing natural killer cell-mediated lysis of lymphoma cells by combining therapeutic antibodies with CD20-specific immunoligands engaging NKG2D or NKp30. *OncoImmunology* 5: e1058459.
70. Klewinghaus, D., L. Pekar, P. Arras, S. Krah, B. Valldorf, H. Kolmar, and S. Zielonka. 2022. Grabbing the bull by both horns: bovine ultralong CDR-H3 paratopes enable engineering of "almost natural" common light chain bispecific antibodies suitable for effector cell redirection. *Front. Immunol.* 12: 801368.
71. Schiestl, M., T. Stangler, C. Torella, T. Čepeljnik, H. Toll, and R. Grau. 2011. Acceptable changes in quality attributes of glycosylated biopharmaceuticals. *Nat. Biotechnol.* 29: 310–312.
72. Grebenau, R. C., D. M. Goldenberg, C. H. Chang, G. A. Koch, D. V. Gold, A. Kunz, and H. J. Hansen. 1992. Microheterogeneity of a purified IgG1 due to asymmetric Fab glycosylation. *Mol. Immunol.* 29: 751–758.
73. Trabanelli, S., M. F. Chevalier, A. Martinez-Usatorre, A. Gomez-Cadena, B. Salomé, M. Lecciso, V. Salvestrini, G. Verdeil, J. Racle, C. Papayannidis, et al. 2017. Tumour-derived PGD2 and NKp30-B7H6 engagement drives an immunosuppressive ILC2-MDSC axis. *Nat. Commun.* 8: 593.
74. Li, Y., Q. Wang, and R. A. Mariuzza. 2011. Structure of the human activating natural cytotoxicity receptor NKp30 bound to its tumor cell ligand B7-H6. *J. Exp. Med.* 208: 703–714.
75. Joyce, M. G., P. Tran, M. A. Zhuravleva, J. Jaw, M. Colonna, and P. D. Sun. 2011. Crystal structure of human natural cytotoxicity receptor NKp30 and identification of its ligand binding site. *Proc. Natl. Acad. Sci. USA* 108: 6223–6228.
76. Bortoletto, N., E. Scotet, Y. Myamoto, U. D'Oro, and A. Lanzavecchia. 2002. Optimizing anti-CD3 affinity for effective T cell targeting against tumor cells. *Eur. J. Immunol.* 32: 3102–3107.
77. Staflin, K., C. L. Zuch de Zafra, L. K. Schutt, V. Clark, F. Zhong, M. Hristopoulos, R. Clark, J. Li, M. Mathieu, X. Chen, et al. 2020. Target arm affinities determine preclinical efficacy and safety of anti-HER2/CD3 bispecific antibody. *JCI Insight* 5: e133757.
78. Ellerman, D. 2019. Bispecific T-cell engagers: towards understanding variables influencing the in vitro potency and tumor selectivity and their modulation to enhance their efficacy and safety. *Methods* 154: 102–117.
79. Burke, J. D., and H. A. Young. 2019. IFN-γ: a cytokine at the right time, is in the right place. *Semin. Immunol.* 43: 101280.
80. Alspach, E., D. M. Lussier, and R. D. Schreiber. 2019. Interferon γ and its important roles in promoting and inhibiting spontaneous and therapeutic cancer immunity. *Cold Spring Harb. Perspect. Biol.* 11: a028480.
81. Ivashkiv, L. B. 2018. IFNγ: signalling, epigenetics and roles in immunity, metabolism, disease and cancer immunotherapy. *Nat. Rev. Immunol.* 18: 545–558.
82. Castro, F., A. P. Cardoso, R. M. Gonçalves, K. Serre, and M. J. Oliveira. 2018. Interferon-gamma at the crossroads of tumor immune surveillance or evasion. *Front. Immunol.* 9: 847.
83. Overacre-Delgoffe, A. E., M. Chikina, R. E. Dadey, H. Yano, E. A. Brunazzi, G. Shayan, W. Horne, J. M. Moskovitz, J. K. Kolls, C. Sander, et al. 2017. Interferon-γ drives T_{reg} fragility to promote anti-tumor immunity. *Cell* 169: 1130–1141.e11.
84. Groom, J. R., and A. D. Luster. 2011. CXCR3 ligands: redundant, collaborative and antagonistic functions. *Immunol. Cell Biol.* 89: 207–215.
85. Melero, I., A. Rouzaut, G. T. Motz, and G. Coukos. 2014. T-cell and NK-cell infiltration into solid tumors: a key limiting factor for efficacious cancer immunotherapy. *Cancer Discov.* 4: 522–526.
86. Sharma, P., and J. P. Allison. 2020. Dissecting the mechanisms of immune checkpoint therapy. *Nat. Rev. Immunol.* 20: 75–76.
87. Sharma, P., and J. P. Allison. 2015. The future of immune checkpoint therapy. *Science* 348: 56–61.